

Appropriate Luminance for Estimating Vegetation Index from Digital Camera Images

Keiji OSAKI

Abstract: It was revealed that estimated vegetation indices with a commercial digital camera have shown anomalously high values over 0.9 in NDVI (Normalized Difference Vegetation Index) for a shady area of the camera images. It was manifested that an exclusion of pixels of the camera image with luminance below a threshold is a key method to remove the shady area and to acquire much better estimation of vegetation index. Appropriate luminance for the purpose requires us to exclude pixels of the image with luminance below about 70 out of 255. Successful removal of shady/anomalous *NDVI* areas and excellent estimation of vegetation index from the images of the specific digital camera were obtained.

Key words: Digital camera images, Estimated NDVI, Light exposure, Luminance, Spectral photometer

1. Introduction

Spectral vegetation indices are derived from quantities in different spectral bands, mostly in visible and near-infrared regions of the spectrum¹⁾. A relationship of visible red and near-infrared reflected light energy is related to the amount of vegetation present on the ground²⁾. The healthy plant absorbs most of the visible light and reflects a large portion of the near-infrared light. On the other hand, unhealthy or sparse plant reflects more visible light and less near-infrared light³⁾. Vegetation indices have been used over a wide range of applications: such as vegetation monitoring, climate and hydrologic modelling, agricultural activities, drought studies and health issues.

Among many proposed vegetation indices, the most widely used vegetation index is the NDVI (Normalized Difference Vegetation Index) which consists of a normalized ratio of near-infrared and visible red reflectance due to NDVI's simplicity and ease of application.

The general usefulness of NDVI is easily found on enormous Web sites in the world. In Australia, "Monthly *NDVI* Average for Australia" has been publicized to everyone as one of climate maps by an official bureau of meteorology⁴⁾.

In India, land use classes of study area are available for better crop efficiency using *NDVI* derived from Indian Remote Sensing Satellite and other earth observation satellites⁵⁾.

To date, NDVI has been widely employed in the estimation of biomass for more than 30 years. This may then provide information on a variety of key terrestrial variables for global environmental issues⁶⁾. Recently proximal remote sensing technologies have come to draw particular attention with the advent of smaller equipment like 'drone camera'⁷⁾.

It is highly expected that a vast potential for practical use of commercial digital cameras as a sort of sensor will increase according as an advancement of mobile technologies' performance. Practical use of digital cameras as one of the tools for a monitoring vegetation property of plants is now prevailing and has been actively investigated^{8,9)}.

It has been called people's attention that two images in near-infrared and visible red bands can produce an estimation of vegetation index with the digital cameras¹⁰⁾. However, it was revealed that the estimated vegetation index with the specific digital cameras show anomalously high values over 0.9 in *NDVI* for shady areas of the captured images¹¹⁾. To achieve higher accuracy of the estimated vegetation index from the camera images, it is unavoidable to deal with the shady areas of the images in an appropriate way.

A necessary evaluation of the accuracy of estimated *NDVI* has been done by comparing with calculated *NDVI* from measured reflectance by using a spectral-radiometer.

Primary goals of this research are to clarify the cause of anomalously high values in *NDVI* estimated from the camera images and to aim at a more accurate estimation of *NDVI*.

2. Anomalously High Vegetation Index

Vegetation shows a unique signature in its reflectance spectrum as shown in Fig. 1. Its reflectance spectrum marks transition zone from absorption by chlorophyll in the visible red region to scatter due to a leaf's internal structure in the Nir (near-infrared) region. From the feature of transition, the most widely used NDVI (Normalized Difference Vegetation Index) is defined by the following Eq. (1).

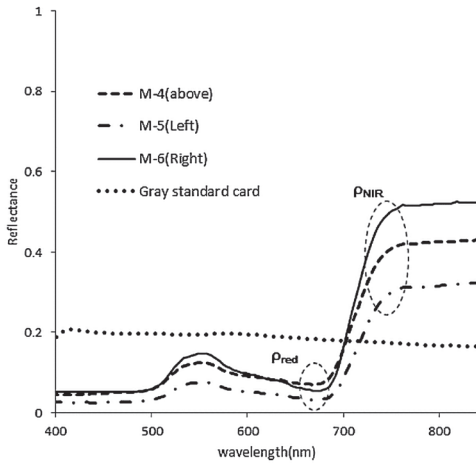


Fig. 1 Spectral reflectance for green leaves: Legend shows three directions of measurement under sunlight by spectral photometer, the three directions will appear in the following Fig. 8. ρ_{Nir} and ρ_{red} are reflectance in near-infrared and visible red bands, respectively. Measured reflectance of gray standard card by spectral photometer under sunlight is shown by dotted line.

$$NDVI = (\rho_{Nir} - \rho_{red}) / (\rho_{Nir} + \rho_{red}) \tag{1}$$

, where ρ_{Nir} and ρ_{red} are reflectance of objects for near-infrared and visible red band, respectively.

Usually, other quantities closely related to the reflectance are often adopted to derive *NDVI* such as radiance, irradiance, luminance, illuminance, etc. because of a difficulty of direct measurement of reflectance. Mathematically values of *NDVI* calculated by Eq. (1) result in a number that ranges from -1 to +1. For objects on the surface of the land, the *NDVI* ranges from values close to 0 for arid or barren areas to about 1 for densely vegetated areas. For water surfaces, the *NDVI* approaches -1 due to their very low reflectance in the Nir band.

Most of the researchers in the remote sensing field have quoted an article by J. Weier and D. Herring about a range of *NDVI* values¹²⁾. It says that an *NDVI* close to 0 corresponds to no vegetation, while *NDVI* close to +1 (0.8 - 0.9) indicates the highest possible density of green leaves. Though one of those researchers concluded that essentially vegetation values have a range from 0.1 to 0.7¹³⁾, it seems to be necessary for further investigation.

From various papers and publicized materials on Web sites, it is reasonable that values of *NDVI* for vegetation lie below 0.8. However, the author has noticed that *NDVI* estimated from the images of the specific camera in near-infrared and visible red bands sometimes show anomalously high values of *NDVI* under a particular condition of light exposure¹¹⁾. Anomalously high values of *NDVI* (>0.9) have appeared in shady or darkest areas of visible photo images.

Here, we need to draw careful attention to the expression, 'anomalous or anomaly' regarding *NDVI*. Because the phrase 'NDVI anomalies' have been frequently used in lots of research articles as deviations of *NDVI* values from a long-term average of *NDVI*. For example, *NDVI* anomalies that were more than one standard deviation below 21-year average conditions, and in 2002, fully 95% of North America exhibited below-average *NDVI*¹⁴⁾.

The term 'anomalous or anomaly' used in this paper signifies that

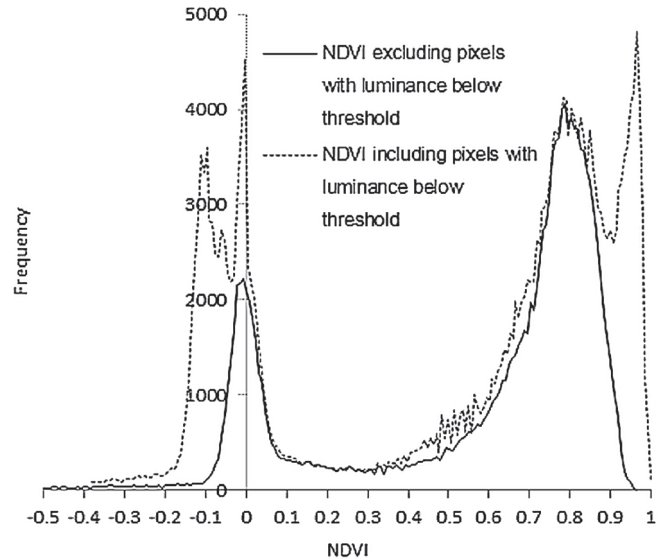


Fig. 2 Histogram of anomalously high values of estimated *NDVI*. Anomalous values signify that *NDVI* values are more than 0.9.

the values of *NDVI* are over 0.9. Distribution of anomalous *NDVI* estimated from captured images is clearly manifested in a histogram as in Fig. 2. It was speculated that the anomalous situation would be caused by insufficient light exposure just like 'under-exposure' in photography.

3. Method for Estimating Vegetation Index from Images

One of the most used vegetation indices is *NDVI* just mentioned in the previous chapter. Two types of images acquired by digital cameras are necessary for estimation of vegetation index from camera images: one is visible band photo, and the other is near-infrared band photo captured with an infrared lens filter. A flow of estimation of vegetation index is shown in Fig. 3. And also to evaluate an accuracy of the estimated *NDVI* from the images, quantity concerning reflectance measured by a spectral photometer is needed as a criterion for the evaluation of the estimated *NDVI*.

It is important to understand a relationship between reflectance of objects and output of the digital camera. Acquiring various spectral/colorimetric quantities is very complicated. However, it is beneficial to review travel of light from incident light to an image sensor of the digital camera as a flow diagram in Fig. 4.

With a spectral photometer, *NDVI* can be directly calculated from a measured reflectance or certain quantity closely related to the reflection unlike the estimation of *NDVI* from captured images.

In remote sensing with a multispectral sensor on platforms of earth observation satellites, the spectral radiance at the top of the atmosphere is acquired at the altitude from the ground surface ranging from 700 km to 450 km. Regarding long-distance view, technologies of proximal remote sensing have emerged to offer enough ground-truth for calibrating data from satellite sensors. We have developed an in-situ measurement of vegetation at a closer distance than proximal remote sensing by the spectral photometer, agricultural digital cameras and commercial digital cameras. In Table 1, a list of items is shown for measurement of radiance and capturing

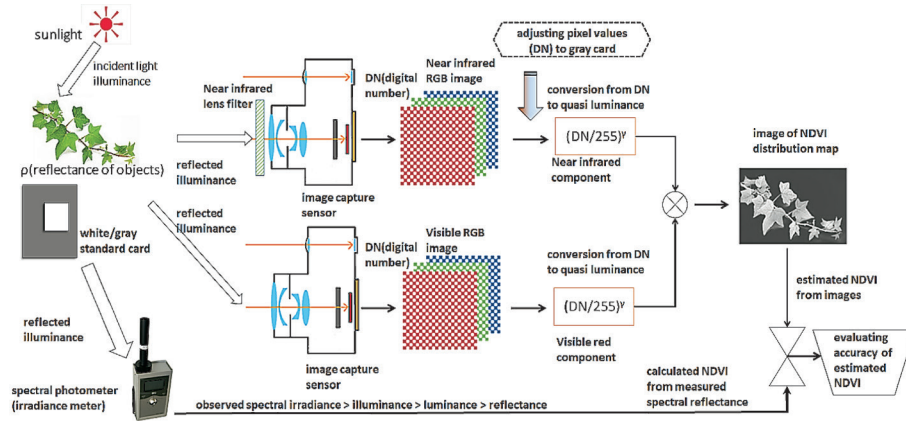


Fig. 3 Flow of estimating vegetation index from captured images by digital camera.

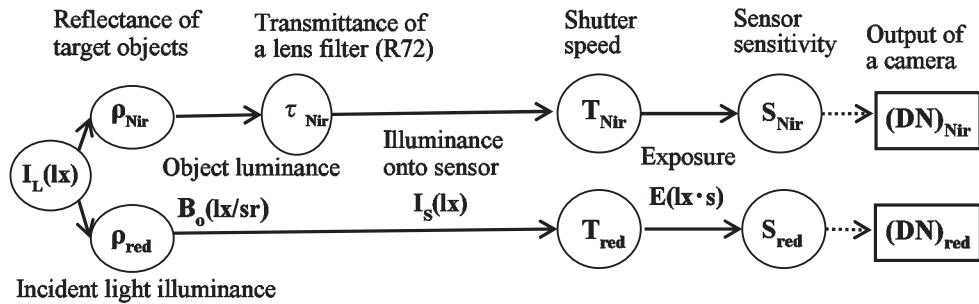


Fig. 4 Traveling of light from light source to image sensor of digital camera

Table 1 Specification of items for measurement of irradiance/radiance and capturing images

Item	For use	Specification
Infrared lens filter	Blocking visible light	Kenko Tokina PRO1D R72 ¹⁹⁾
Artificial sunlight lamp	Emitting sunlight	SERIC SOLAX XC-100AF ²¹⁾
Portable spectral photometers	Measuring radiance/irradiance	FieldSpec HH ²⁰⁾ EIKO MS-720
Color chart	Calibration of radiance	gmb ColorChecker
LCD display	Displaying digital images	EIZO FlexScan L887
Plants (Outdoor place)	Target objects for images under sunlight	Hedera, turf, field weeds (Tokyo) Wild buckwheat (Akita) Shrubs (Tokyo, Kushiro) Weeds (Nagasaki)
Plants (Indoor)	Target objects for images under the artificial sunlight	Potted Hedera Pittsburgh
Agricultural digital cameras	Comparison of vegetation indices	Tetracam ADC-3 BIZWORKS Yubaflex
Commercial digital cameras	Capturing digital images Recording geolocation data	CANON Powershot 710IS CANON S110 OLYMPUS C-5060 CASIO EX-H20G

camera images.

The table also indicates several target plants in various places for observation. To clarify the optical properties of the visible light blocking filter 'R72', the spectral transmittance curves of the 'R72'

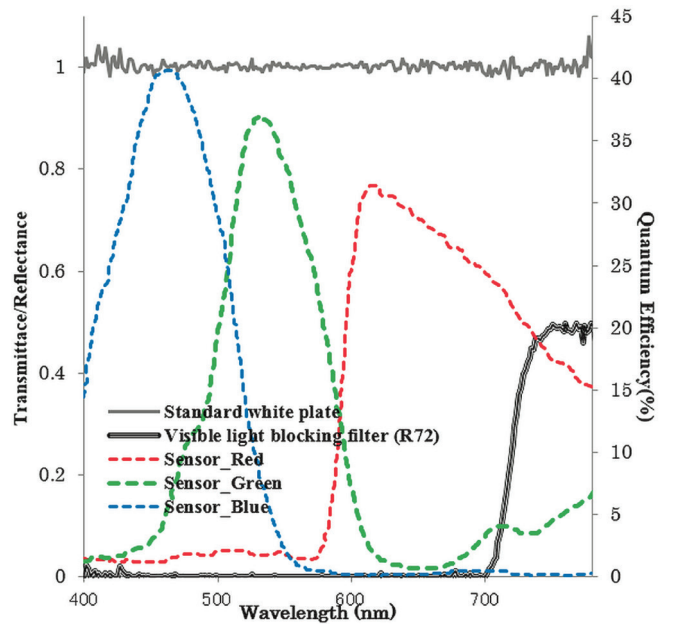


Fig. 5 Spectral quantum efficiency of an image color sensor and measured spectral reflectance of standard white plate and transmittance of visible light blocking filter, 'R72' by the spectral photometer, 'FieldSpec HH' under the artificial sunlight, 'SOLAX XC-100AF'. Spectral characteristics curves of the image color sensor, 'KAI-0340'²²⁾ as a typical example of CCD sensor are shown in quantum efficiency (%) of right axis.

and the spectral characteristics curves of the CCD camera sensor are shown in Fig. 5.

The primary purpose of our research is to develop the method for

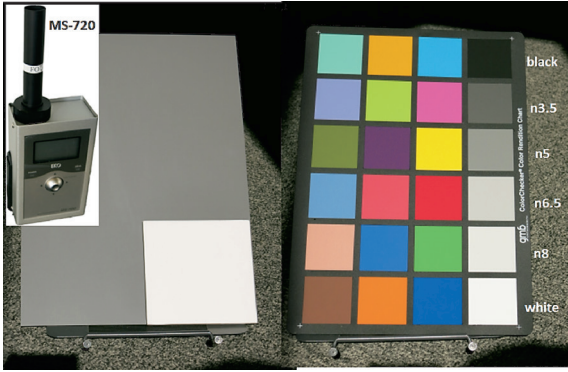


Fig. 6 Spectral photometer (MS-720), white reference card and color- rendition card (ColorChecker Classic)^{17,18)}: Various gray-level patches are for irradiance calibration of the photometer.

higher accurate estimation of *NDVI* from the images by the commercial digital camera. To achieve it, we have selected 'CANON 710IS' as the choice digital camera and 'Potted Hedera Pittsburgh' as the plant with high *NDVI* value among many cases. Since the size and shape of leaves of 'Wild buckwheat' are similar to those of the 'Potted Hedera', we compared the difference of vegetation map between outdoor and indoor measurements with the images of 'Wild buckwheat'²³⁾.

Regarding two agricultural digital cameras, they have marked poorer results of evaluation of estimated vegetation map from their camera images than the results from the 'CANON 710IS'.

A portable spectral photometer 'MS-720' seen in Fig. 6 has been used to calculate *NDVI* from its measured output.

Though the output of MS-720 is irradiance (W/m^2) of target objects, the output can be approximately transformed to radiance ($W/m^2/sr$) because FOV (Field of View) of the photometer is 10 degrees and sufficiently small. Then, a ratio of the irradiances is closely related to the reflectance of the target objects.

We approximate spectral sensor output of the digital camera by the following equations as DN (Digital Number):

$$\begin{aligned} (DN)_{Nir} &= K_{Nir} \sum_{\lambda} [I_L(\lambda) \cdot \rho_{Nir}(\lambda) \cdot \tau_{Nir}(\lambda) \cdot T_{Nir} \cdot S_{Nir}(\lambda)] \\ (DN)_{red} &= K_{red} \sum_{\lambda} [I_L(\lambda) \cdot \rho_{red}(\lambda) \cdot T_{red} \cdot S_{red}(\lambda)] \end{aligned} \quad (2)$$

, where K is a ratio of camera output to light exposure, I_L is an incident light illuminance[lx], ρ is a reflectance of a target object, τ is a transmittance of a lens filter, T is a shutter speed, S is a sensor sensitivity, respectively.

Since the ratio of irradiance is proportional to that of reflectance of objects, measured irradiance by spectral photometer with small FOV can be used for calculation of *NDVI*.

4. Appropriate Light Exposure for Estimating *NDVI* and Results

According to famous paper "A Color-Rendition Chart"¹⁸⁾, each patch is characterized by spectral reflectance factor; assigned name; CIE (1931) x , y , and Y ; Munsell notation (λ); and ISCC-NBS name. Recently, various charts for color calibration and other purposes are issued in addition to the classical color chart¹⁷⁾. Measured irradiance

Table 2 Reflectance of gray scale patches from "ColorCheckerClassic"^{17,18)} and measured irradiance by the portable spectral photometer (MS-720).

ColorChecker Classic	Munsell Value	% Reflect.	Measured Irradiance (W/m ² m)
Black	2.00	3.10	0.047
N3.5	3.50	9.00	0.154
N5	5.00	19.77	0.316
N6.5	6.50	36.20	0.617
N8	8.00	59.10	0.983
White	9.50	90.01	1.640

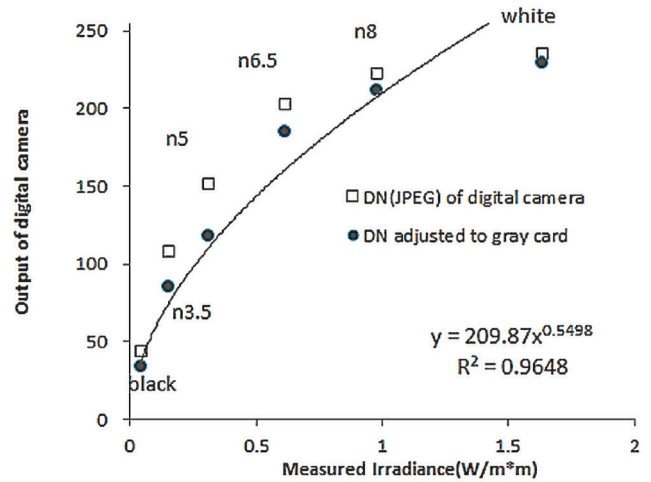


Fig. 7 Digital camera's output against measured irradiance by the spectral photometer.

by MS-720 is precisely proportional to the luminous reflectance factor (% Reflect.) as seen in Table 2. Thus, the linearity of the MS-720's output to input light is considered to be guaranteed.

Based on the linearity of the MS-720, the spectral reflectance of the standard gray card was measured and is plotted by the dotted line in Fig. 1. The reflectance of the standard gray card shows nearly 20% of the visible light wavelength.

On the other hand, DN values of patch images captured by a digital camera (e.g. CANON S110) show a power-law to the measured irradiance by the photometer as in Fig. 7. By fitting a curve to DN adjusted to gray card, its exponent of the power-law was found to be 1.82 (=1/0.5498).

Among two captured images by the digital camera, the visible light image is displayed with three directions for spectral measurement by the MS-720 in Fig. 8. The ellipse in orange color indicates target areas used for estimating *NDVI* from the images. The image also shows a white reference card and a standard gray card. It is apparent that shady or darkest areas are seen in various regions in Fig. 8. It was revealed that these shady areas and areas that showed anomalously high values of *NDVI* almost overlapped.

Since luminance of the captured image is closely related to light exposure onto the image capture sensor in Fig. 3, it might be expected that a specific feature of anomalous *NDVI* will appear in a scatterplot between a luminance of the image and estimated *NDVI* from the images. As the characteristics of the scatterplots are indicated in Fig. 9, a distinct region showing anomalously high values of *NDVI* (>0.9) appears bottom right in the figure. This area is abnormal for

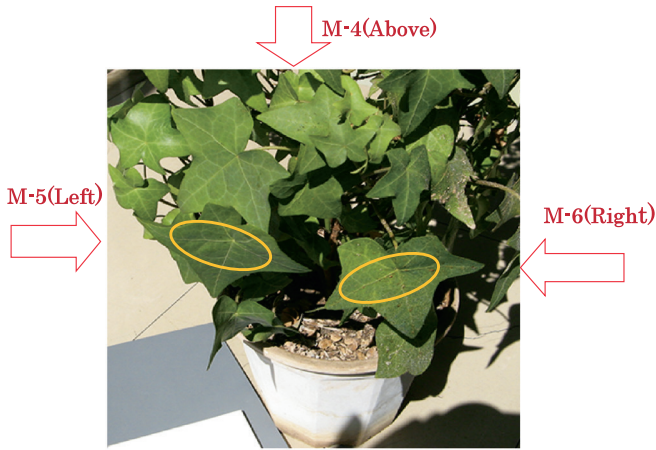


Fig. 8 Visible light image captured by a digital camera under sunlight. Target areas of the image for estimating *NDVI* are shown by orange ellipse with its height of 1.5cm and width of 3 cm.

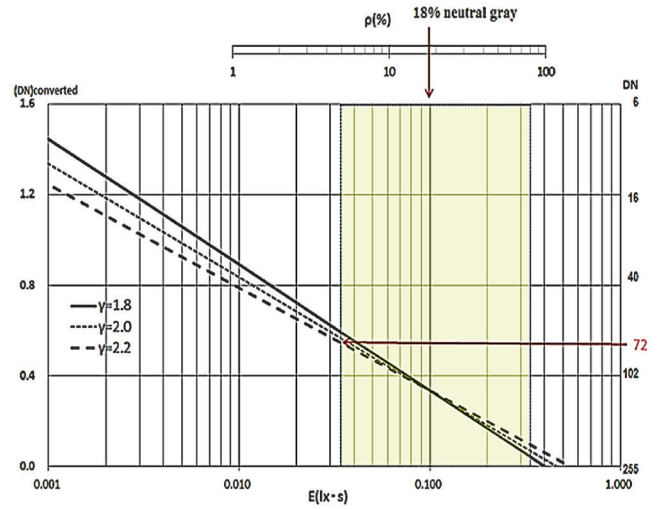


Fig. 10 Converted output of the digital camera image against light exposure of the camera image sensor. Threshold value of the output *DN* of 72 for exclusion of the pixels exposure is indicated by a red arrow. Gray standard is also indicated as '18% neutral gray' corresponding to the exposure of 0.100(lx·s)^{15,16}.

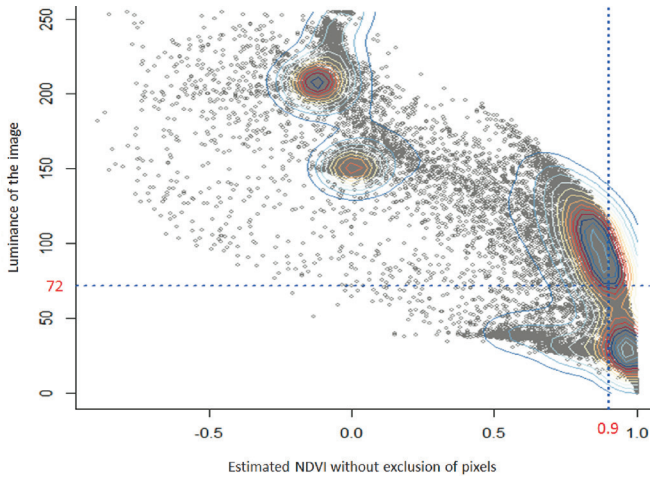


Fig. 9 Scatterplots between luminance of the camera image and estimated *NDVI* from the camera images. Number of plotted pixels are randomly sampled from 512x512 to 24,000. Contour lines in the figure show high density of aggregated pixels and threshold luminance of 72 and *NDVI* of 0.9 are indicated in red letters.

the estimated *NDVI*; therefore it has to be excluded for an accurate estimation.

Then, it was discovered that a threshold of light exposure E (lx·s) gave a threshold value of luminance for anomalous *NDVI*. It corresponds to a threshold value of *DN* (=72) in luminance calculated from the camera image. Thus, the luminance threshold value of the visible color image is utilized for removal of the shady area from the estimation process of *NDVI*.

Fig. 10 indicates us an appropriate light exposure for estimation of *NDVI* from digital camera images. It signifies that E (lx·s) > 0.033 or $DN > 72$ for gamma of 2.2, where $(DN)_{converted}$ is defined by $-\log_{10}(DN/255)^{\gamma}$.

Appropriate light exposure for capture of photo images can give more precise estimation of *NDVI* from near-infrared and visible red images. The following equation gives luminance Y' from R' , G' , and B' of camera images:

$$Y' = 0.2999R' + 0.567G' + 0.114B' \text{ (NTSC-TV)}, \quad (3)$$

where prime indicates gamma-corrected R , G , B .

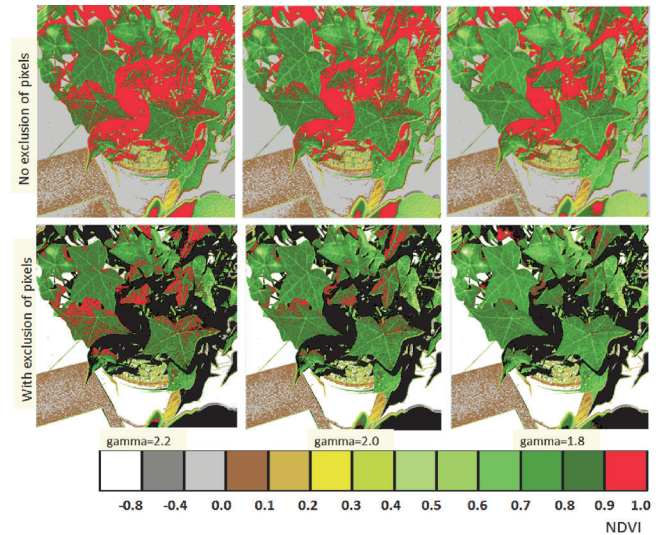


Fig. 11 Distribution map of anomalous *NDVI* region shown in red area. It is shown that variation of area of pixels with anomalous *NDVI* (>0.9) depends on gamma values. Upper three colored maps are derived by no exclusion of pixels with luminance below threshold. Lower three colored maps are derived by excluding pixels whose luminance lies below 72.

While the *NDVI* calculated from measured quantity by spectral photometer has a limited scope, the *NDVI* estimated from the images can cover a spacious sphere and it is one of the surpassing advantages. In Fig. 11, a distribution map of the estimated *NDVI* is displayed as level-sliced color images. It is shown that area with anomalous *NDVI* changes depending on gamma values.

When anomaly of *NDVI* is defined by the ratio of pixels with $NDVI > 0.9$ to total pixels of the estimated *NDVI* map image, it is manifested that anomaly ratio of the estimated *NDVI* changes in an almost linear way to gamma values.

As seen in Fig. 12, anomaly ratio of the *NDVI* remains 7.0% for gamma=2.2 even in the case of excluding pixels with luminance be-

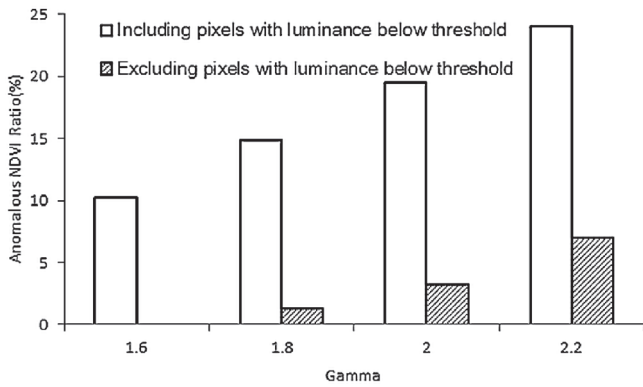


Fig. 12 Dependence of anomaly ratio of the *NDVI* on the gamma values

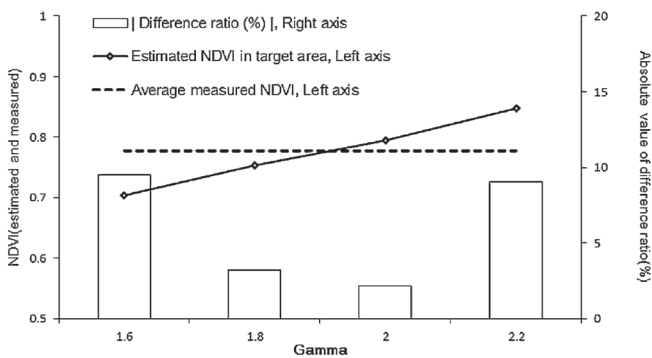


Fig. 13 Comparison of the estimated *NDVI* from the camera images with measured *NDVI* derived from the irradiance acquired by the spectral photometer: Dependence of estimated *NDVI* on the gamma values is shown.

low the threshold. For gamma=1.8 anomalous area of *NDVI* shrinks to 1.33. It is a drastic improvement for estimating *NDVI* from the camera images. As previously mentioned in the paragraph referring to Fig. 7, the exponent of the power-law for the curve was 1.82. It is manifested that the proper value of gamma for the output of the digital camera might be 1.8 when we use the camera as a certain kind of a photometer.

For evaluation of the accuracy of the estimated *NDVI* from the camera images, it is important to compare the estimated *NDVI* with the *NDVI* calculated from measured reflectance by the spectral photometer. In Fig. 13, the comparison is shown by using an absolute value of difference ratio between the estimated and the calculated *NDVI*.

To evaluate an accuracy of the estimation of *NDVI* from camera images, target area where the photometer points from a distant of about 20 cm or so was selected on the surface of a leaf as indicated by an orange ellipse in Fig. 8. Taking the corresponding target area of the photo image, the estimated *NDVI* was obtained by averaging the *NDVI* values within the target area.

The result is given for comparison in Fig. 13 and explained in detail as follows.

A difference of *NDVI* between estimated *NDVI* from images and average of measured *NDVI*s (*M-4*, *M-5* and *M-6* in Fig. 8) varies depending on the gamma values. The absolute value of difference ratio (%) lies from 2 to 3% for gamma near 1.8. It can be said that the proposed pixel exclusion method results in better and excellent

estimation of *NDVI* from the digital camera images.

5. Conclusion

Current research showed excellent features by the method of excluding pixels with luminance below the threshold from estimating *NDVI* from the specific camera images.

Proposed criterion of the appropriate light exposure for the *NDVI* estimation is that light exposure lies more than 0.033 (lx·s). It corresponds to that the luminance of the image should be more than 72 out of 255 for the gamma of 2.2.

The ratio of a difference between the estimated *NDVI* from the camera images and calculated one by the measured reflectance stays within about 3%.

For the purpose of utilizing digital cameras like some photometer, it might be recommended to set gamma to 1.8 rather than 2.2 during the image processing for *NDVI* estimation.

Acknowledgement

This work was supported by JSPS KAKENHI Grant Number 26450367. Grant-in-Aid for Scientific Research (C)

References

- 1) Wu, Weicheng. "The generalized difference vegetation index (GDVI) for dryland characterization." *Remote Sensing* 6(2), 1211-1233 (2014).
- 2) Bannari, A. et al. "A review of vegetation indices." *Remote sensing reviews* 13.1-2, 95-120 (1995).
- 3) Abraham, Lizy and Sasikumar, M. "Unsupervised building extraction from high resolution satellite images irrespective of rooftop structures." *International Journal of Image Processing (IJIP)* 6.4, 219-232 (2012).
- 4) Australian Government Bureau of meteorology: "Monthly *NDVI* Average for Australia" <http://www.bom.gov.au/jsp/awap/ndvi/index.jsp> [Accessed on Aug. 23, 2015].
- 5) Murali, Krishna Gumma et.al. *Crop Dominance Mapping with IRS-P6 and MODIS 250-m Time Series Data*, *Agriculture* 4(2), 113-131 (2014).
- 6) Foody, G. M. "Remote sensing of tropical forest environments: towards the monitoring of environmental resources for sustainable development." *International journal of remote sensing* 24.20, 4035-4046 (2003).
- 7) Rasmussen, Jesper; Nielsen, J.; Garcia-Ruiz, F.; Christensen, S and Streibig, J C "Potential uses of small unmanned aircraft systems (UAS) in weed research." *Weed Research* 53.4, 242-248 (2013).
- 8) Li, Y. et al. "Estimating the nitrogen status of crops using a digital camera." *Field Crops Research* 118.3, 221-227 (2010).
- 9) Lebourgeois, Valentine et al. "Can commercial digital cameras be used as multispectral sensors? A crop monitoring test." *Sensors* 8.11, 7300-7322 (2008).
- 10) Osaki, Keiji "Evaluation of Vegetation Index Derived from Digital Camera's Images." *Journal of the Imaging Society of Japan* 51(2), 118-124, (2012).
- 11) Osaki, Keiji "Characteristics of Green Normalized Difference Vegetation Index Calculated from Images by Commercial Digital Camera." *Imaging Conference Japan fall meeting*, 67-70 (2013).
- 12) Weier, John and Herring, David "Measuring Vegetation." 2000. <http://earthobservatory.nasa.gov/Features/MeasuringVegetation/> [Accessed on Aug.23, 2015]
- 13) Tagil, Sermin "Monitor Land Degradation Phenomena Through Land-

- scape Metrics and NDVI" *Journal of Applied Sciences* 7(14),1827-1842 (2007).
- 14) Chretien, Jean-Paul et al. "Drought-associated chikungunya emergence along coastal East Africa." *The American journal of tropical medicine and hygiene* 76.3, 405-407 (2007).
 - 15) Yoshida, Hideaki "3. Evaluation Methods of Characteristics and Image Quality for Home-use Cameras (<Special Edition>Progress on Technologies for Higher Image Quality and Image Quality Assessment of Cameras and Displays for Consumer Use)." *The Journal of the Institute of Image Information and Television Engineers* 63.6, 735-740 (2009).
 - 16) CIPA, "CIPA DC-003-Translation-2003 Resolution Measurement Methods for Digital Cameras", Tokyo, 2003. http://www.cipa.jp/english/hyoujunka/kikaku/pdf/DC-003_e.pdf [Accessed on Aug.28, 2015]
 - 17) Myers, Robin D. "Colorchecker passport technical review." *Robin Myers Imaging* (2010). http://www.rmimaging.com/information/ColorChecker_Passport_Technical_Report.pdf [Accessed on Aug.23, 2015].
 - 18) McCamy, C.S.; Marcus, H. and Davidson, J.G. "A Color-Rendition Chart", *Journal of Applied Photographic Engineering*, Vol.2, 95-99 (1976).
 - 19) Kenko Tokina, "PRO1D R72" [Infrared lens filter], <http://www.kenko-tokina.co.jp/imaging/filter/pro1d/> [Accessed on Nov. 10, 2015].
 - 20) ASD Inc., "FieldSpec HH" [Portable spectral photometer], <http://www.asdi.com/products/fieldspec/handheld-2-pro-vnir-hand-held-spectroradiometer> [Accessed on Nov. 10, 2015].
 - 21) SERIC, "SOLAX XC-100AF" [Artificial sunlight lamp], <http://www.seric.co.jp/product/lig/lig01.html> [Accessed on Nov. 10, 2015].
 - 22) AD Science Inc., "OnSemi KAI-0340" [CCD camera sensor], http://www.ads-img.co.jp/wp-content/uploads/avt_ge_techman.pdf [Accessed on Nov. 10, 2015].
 - 23) Osaki, Keiji "Influences of Shadow Areas on Vegetation Map Estimated from Outdoor Images Captured by a Digital Camera." *Imaging Conference Japan 2014*, 71-74 (2014).